JOURNAL OF THE AMERICAN COLLEGE OF CARDIOLOGY VOL. 73, NO. 2, 2019

PUBLISHED BY ELSEVIER

Comparison of Coronary Computed Tomography Angiography, Fractional Flow Reserve, and Perfusion Imaging for Ischemia Diagnosis

Roel S. Driessen, MD,[a] Ibrahim Danad, MD,[a] Wijnand J. Stuijfzand, MD,[a] Pieter G. Raijmakers, MD, PhD,[b] Stefan P. Schumacher, MD,[a] Pepijn A. van Diemen, MD,[a] Jonathon A. Leipsic, MD,[c] Juhani Knuuti, MD, PhD,[d] S. Richard Underwood, MD, PhD,[e] Peter M. van de Ven, PhD,[f] Albert C. van Rossum, MD, PhD,[a] Charles A. Taylor, PhD,[g,h] Paul Knaapen, MD, PhD[a]

ABSTRACT

BACKGROUND Fractional flow reserve (FFR) computation from coronary computed tomography angiography (CTA) datasets (FFR_{CT}) has emerged as a promising noninvasive test to assess hemodynamic severity of coronary artery disease (CAD), but has not yet been compared with traditional functional imaging.

OBJECTIVES The purpose of this study was to evaluate the diagnostic performance of FFR_{CT} and compare it with coronary CTA, single-photon emission computed tomography (SPECT), and positron emission tomography (PET) for ischemia diagnosis.

METHODS This subanalysis involved 208 prospectively included patients with suspected stable CAD, who underwent 256-slice coronary CTA, 99mTc-tetrofosmin SPECT, [^{15}O]H_2O PET, and routine 3-vessel invasive FFR measurements. FFR_{CT} values were retrospectively derived from the coronary CTA images. Images from each modality were interpreted by core laboratories, and their diagnostic performances were compared using invasively measured FFR ≤0.80 as the reference standard.

RESULTS In total, 505 of 612 (83%) vessels could be evaluated with FFR_{CT}. FFR_{CT} showed a diagnostic accuracy, sensitivity, and specificity of 87%, 90%, and 86% on a per-vessel basis and 78%, 96%, and 63% on a per-patient basis, respectively. Area under the receiver-operating characteristic curve (AUC) for identification of ischemia-causing lesions was significantly greater for FFR_{CT} (0.94 and 0.92) in comparison with coronary CTA (0.83 and 0.81; $p < 0.01$ for both) and SPECT (0.70 and 0.75; $p < 0.01$ for both), on a per-vessel and -patient level, respectively. FFR_{CT} also outperformed PET on a per-vessel basis (AUC 0.87; $p < 0.01$), but not on a per-patient basis (AUC 0.91; $p = 0.56$). In the intention-to-diagnose analysis, PET showed the highest per-patient and -vessel AUC followed by FFR_{CT} (0.86 vs. 0.83; $p = 0.157$; and 0.90 vs. 0.79; $p = 0.005$, respectively).

CONCLUSIONS In this study, FFR_{CT} showed higher diagnostic performance than standard coronary CTA, SPECT, and PET for vessel-specific ischemia, provided coronary CTA images were evaluable by FFR_{CT}, whereas PET had a favorable performance in per-patient and intention-to-diagnose analysis. Still, in patients in whom 3-vessel FFR_{CT} could be analyzed, FFR_{CT} holds clinical potential to provide anatomic and hemodynamic significance of coronary lesions.
(J Am Coll Cardiol 2019;73:161–73) © 2019 by the American College of Cardiology Foundation.

Listen to this manuscript's audio summary by Editor-in-Chief Dr. Valentin Fuster on JACC.org.

From the [a]Department of Cardiology, VU University Medical Center, Amsterdam, the Netherlands; [b]Department of Radiology, Nuclear Medicine & PET Research, VU University Medical Center, Amsterdam, the Netherlands; [c]Department of Medicine and Radiology, University of British Columbia, Vancouver, British Columbia, Canada; [d]Turku PET Centre, Turku University Hospital and University of Turku, Turku, Finland; [e]Department of Nuclear Medicine, Royal Brompton Hospital, London, United Kingdom; [f]Department of Epidemiology and Biostatistics, VU University Medical Center, Amsterdam, the Netherlands; [g]HeartFlow, Inc., Redwood City, California; and the [h]Department of Bioengineering, Stanford University, Stanford, California. Dr. Leipsic has received research grants from GE Healthcare; and serves as a consultant and holds stock options in Circle CVI and HeartFlow. Dr. Knuuti has provided trial consultancy for GE Healthcare and AstraZeneca. Dr. Underwood provides occasional consultancy to

ISSN 0735-1097/$36.00 https://doi.org/10.1016/j.jacc.2018.10.056

ABBREVIATIONS AND ACRONYMS

CTA = computed tomography angiography

FFR = fractional flow reserve

FFR_{CT} = fractional flow reserve derived from coronary computed tomography angiography

ICA = invasive coronary angiography

PET = positron emission tomography

SDS = summed difference scores

SPECT = single-photon emission computed tomography

At present, a large armamentarium of noninvasive tests is available to diagnose coronary artery disease (CAD) and subsequently risk stratify patients or guide revascularization options (1,2). The importance of accurately using these noninvasive tests is highlighted by the present-day low diagnostic yield of invasive coronary angiography (ICA) (3) and is emphasized by current guidelines for the management of suspected stable CAD (4,5). Among the available modalities, coronary computed tomography angiography (CTA) is an established diagnostic tool that strongly correlates with ICA (6). However, the estimation of hemodynamic significance by anatomic stenosis severity, as determined with coronary CTA as well as with ICA, has shown to be unreliable (7,8). This shortcoming of visual assessment of lesion severity is emphasized by previous studies, which showed that event-free survival was not improved by revascularization based on invasive angiography alone, but it did improve when invasive angiography was combined with physiological measures in terms of invasive fractional flow reserve (FFR) (9). As such, FFR has emerged as the gold standard for determining lesion-specific ischemia and guiding revascularization decision making. Conversely, myocardial perfusion imaging (MPI) with single-photon emission

SEE PAGE 174

computed tomography (SPECT) or positron emission tomography (PET) provides physiological repercussions of CAD at the myocardial tissue level, but lacks coronary anatomical information. Recently, fractional flow reserve derived from computed tomography (FFR_{CT}) has emerged as a promising alternative, providing functional significance of CAD derived from a standard coronary CTA (10). Using computational fluid dynamics, pressures during simulated stress can be calculated, which allows for an assessment of physiological significance of CAD expressed as FFR. Previous prospective trials have shown a significant improvement of diagnostic power for FFR_{CT} in comparison with coronary CTA stenosis assessment alone (11–13). Comparative studies investigating FFR_{CT} against other functional imaging modalities, however, are lacking. Therefore, the aim of this PACIFIC (Prospective Comparison of Cardiac PET/CT, SPECT/CT Perfusion Imaging and CT Coronary Angiography With Invasive Coronary Angiography) trial (14) substudy was to evaluate the diagnostic performance of FFR_{CT} and compare it with coronary CTA, SPECT, and PET for the diagnosis of ischemia.

METHODS

PATIENT POPULATION. This post hoc substudy comprised all 208 patients from the PACIFIC trial who were suspected of CAD and who underwent coronary CTA, SPECT, and PET with routine interrogation by FFR of all major coronary arteries (NCT01521468) (14). In this single-center study, all patients prospectively underwent all noninvasive imaging and ICA with FFR within 2 weeks, regardless of the imaging results. Participants were characterized by an intermediate pre-test likelihood of stable CAD and normal left ventricular ejection fraction (LVEF). Patients were not eligible if they had previously documented CAD, signs of prior myocardial infarction, atrial fibrillation, renal failure, or contraindications to adenosine. The study complied with the Declaration of Helsinki, the study protocol was approved by the VUmc Medical Ethics Review Committee, and all patients provided written informed consent.

CORONARY CTA. Coronary CTA was performed using a 256-slice CT scanner (Philips Brilliance iCT, Philips Healthcare, Best, the Netherlands) as described previously (14) in accordance with the society of cardiovascular computed tomography (SCCT) guidelines (15). Prior to the scanning protocol, sublingual nitroglycerine spray was administered to all patients and metoprolol only if necessary, aiming for a heart rate <65 beats/min. The scan was triggered using an automatic bolus-tracking technique with a region of interest placed in the descending thoracic aorta. Prospective electrocardiogram gating was used at 75% of the R-R interval. Nevertheless, persistent elevated heart rates in 4 scans required a retrospective helical protocol. An intravenous bolus of 100 ml of iodinated contrast agent was injected. Coronary CTA datasets were transmitted to an independent and blinded core laboratory (St. Paul's Hospital, Vancouver, British Columbia, Canada) for the evaluation of diameter stenosis severity. All coronary segments ≥2 mm in diameter were visually graded on

GE Healthcare. Dr. Taylor has an equity interest in and is an employee of HeartFlow. Dr. Knaapen has received unrestricted research grants from HeartFlow. All other authors have reported that they have no relationships relevant to the contents of this paper to disclose.

Manuscript received May 23, 2018; revised manuscript received September 24, 2018, accepted October 8, 2018.

an intention-to-diagnose basis and classified as 0%, 1% to 24%, 25% to 49%, 50% to 69%, and 70% to 100% diameter stenosis, whereas stenosis ≥50% or unevaluable segments were considered significantly obstructive.

FFR DERIVED FROM COMPUTED TOMOGRAPHY. FFR_{CT} technology involves extraction of a patient-specific geometric model of the coronary arteries from coronary CTA data, population-derived physiological models, and computational fluid dynamics techniques to solve the governing equations of blood flow for velocity and pressure under simulated hyperemic conditions (10). In this study, updated FFR_{CT} software was used (HeartFlow FFR_{CT} version 2.7, Redwood City, California), comprising deep-learning artificial intelligence methods to aid in identifying the lumen boundary, physiological models incorporating vessel lumen volume as well as myocardial mass data and hybrid 3-dimensional-1-dimensional computational fluid dynamics methods to improve computational efficiency while maintaining accuracy (16). HeartFlow first performed an image quality check with rejection of uninterpretable cases because of incompletely imaged myocardium or coronary arteries (partly outside of field of view) or severe forms of misalignment, motion, blooming, noise, or other artifacts, followed by FFR_{CT} analysis blinded to the other imaging reads as well as the invasive angiographic and FFR data. Extraction of FFR_{CT} values was performed by an independent researcher (R.D.) with knowledge of the FFR wire position but not invasive FFR values. FFR_{CT} ratios could be obtained along the entire epicardial tree, but were taken at the same position as the FFR wire, which was generally in the distal part of the vessel and not at a specific post-stenosis location, as per PACIFIC study protocol. For identified occluded coronary arteries, a value of 0.50 was assigned.

MPI WITH SPECT. MPI with SPECT was acquired and analyzed as reported previously (14). In summary, SPECT images were acquired on a dual-head hybrid SPECT/CT scanner (Symbia T2, Siemens Medical Solutions, Erlangen, Germany). All patients underwent a 2-day stress-rest 99mTc-tetrofosmin protocol using intravenous adenosine (140 μg/kg/min) as a hyperemic agent and a weight-adjusted dose of 370 to 550 MBq 99mTc-tetrofosmin as radiotracer. All SPECT images were acquired using electrocardiographic gating and followed by a low-dose CT scan for attenuation correction. Image analysis was performed by a blinded core laboratory (Royal Brompton Hospital, London, England). MPI images were interpreted based on a 17-segment model. Each segment was scored using a 5-point scoring system (0, normal; 1, mildly decreased; 2, moderately decreased; 3, severely decreased; and 4, absence of segmental uptake). Summed rest scores, summed stress scores, and summed difference scores (SDS) were calculated from the segmental scores, with an SDS ≥2 considered abnormal.

MPI WITH PET. PET scans were performed using a hybrid PET-CT device (Philips Gemini TF 64, Philips Healthcare). Acquisition and analysis of PET imaging were described previously (14). In short, a dynamic PET perfusion scan was performed using 370 MBq of [^{15}O]H_2O during resting and adenosine (140 μg/kg/min)-induced hyperemic conditions. Low-dose CT scans allowed for attenuation correction. Reconstructed images were sent to a blinded core laboratory (Turku University Hospital, Turku, Finland), where images with quantitative myocardial blood flow (MBF) were generated. Hyperemic MBF, expressed in ml/min/g of perfusable myocardial tissue, was calculated for all 3 vascular territories derived from standard segmentation: left anterior descending, left circumflex, and right coronary artery. Hyperemic MBF ≤2.30 ml/min/g was defined abnormal (17).

ICA AND FFR. ICA was performed using a standard protocol in at least 2 orthogonal directions per evaluated coronary artery segment. For the induction of epicardial coronary vasodilation, 0.2 ml of intracoronary nitroglycerin was administered prior to contrast injection. All major coronary arteries were routinely interrogated by FFR, regardless of stenosis severity, except for occluded or subtotal lesions of more than 90%. Intracoronary (150 μg) or intravenous (140 μg/kg/min) adenosine infusion was used to induce maximal coronary hyperemia. FFR was calculated as the ratio of mean distal intracoronary pressure and mean arterial pressure. A coronary lesion was considered hemodynamically significant in case of FFR ≤0.80, or stenosis severity >90% obtained with quantitative coronary angiography in case of missing FFR. A stenosis with an FFR >0.80 or a stenosis severity <30% (obtained with quantitative coronary angiography) in the absence of FFR measurements was considered not to be functionally relevant. All images and FFR signals were interpreted by experienced interventional cardiologists blinded to imaging results.

STATISTICAL ANALYSIS. Continuous variables are presented as mean ± SD or median (interquartile range) as appropriate. Categorical variables are expressed as frequencies and percentages. Differences between continuous baseline characteristic variables were compared using the 2-sided Student's

TABLE 1 Coronary CTA Assessment Characteristics

	Total Cohort (N = 208)	Primary Analysis Group (n = 157)	Incomplete/Nonevaluable Coronary CTAs (n = 51)	p Value for Subgroups
Heart rate	57.8 ± 7.7	56.5 ± 7.0	61.8 ± 8.3	<0.001
Pre-scan B-blockers	109 (52)	80 (51)	29 (57)	0.002
Pre-scan nitrates	203 (98)	154 (98)	49 (96)	0.415
Prospective acquisition	201 (97)	155 (99)	46 (90)	0.003
CAC score	179 (19–499)	176 (19–485)	236 (6–947)	0.370
Per-vessel CAC score	29 (0–174) 612 vessels	29 (0–160) 505 vessels	19 (0–264) 107 vessels	0.650

Values are mean ± SD, n (%), or median (interquartile range).
CAC = coronary artery calcification; CTA = computed tomography angiography.

t-test, whereas differences between categorical baseline variables were analyzed by the chi-square test or Fisher exact test when appropriate. The study endpoint was the comparison of FFR_{CT} against CT, SPECT, and PET, in terms of sensitivity, specificity, negative predictive value, positive predictive value (PPV), diagnostic accuracy, and area under the receiver operating characteristic curve (AUC), referenced by invasive FFR. In patient-based analysis, these diagnostic measures were calculated as simple proportions with 95% confidence intervals (CIs). In vessel-based analysis, diagnostic measures were calculated using generalized estimating equations (GEE) with an exchangeable correlation structure to account for within-patient correlation. AUCs were generated to quantify the discriminative ability of each modality, and compared using the method of DeLong et al. (18) with MedCalc (MedCalc Software 12.7.8.0, Mariakerke, Belgium). Sensitivity, specificity, and accuracy for diagnosis on a patient level were compared using McNemar's test, whereas PPV and negative predictive value were compared using a marginal regression model using a working independent correlation structure. Patients were considered positive for a modality (reference standard) if at least 1 vessel was considered positive. Vessel-based diagnostic measures were compared using GEE with an exchangeable correlation structure to account for correlation between multiple vessels within the same patient. Primary per-vessel analysis was performed using all vessels that were evaluable by FFR_{CT}, whereas only fully evaluable coronary CTA datasets (i.e., 3-vessel) were used on a per-patient basis. Secondary analysis was performed with all datasets on an intention-to-diagnose (i.e., nonevaluable vessels were deemed positive). The diagnostic performance of combined FFR_{CT} and coronary CTA was explored by including these parameters in a multivariable model using GEE and a subsequent AUC comparison, next to reporting combined FFR_{CT} and CTA results together with other imaging results according to FFR subgroups. The combined FFR_{CT} and coronary CTA was considered positive only when both FFR_{CT} and coronary CTA were positive according to 1 of the 2 coronary CTA thresholds (>25% and >50%). The association between FFR_{CT} and invasive FFR was quantified using Pearson's and Spearman's correlation coefficients and agreement was assessed with Bland-Altman analysis. A p value ≤0.05 was considered statistically significant. All statistical analyses were performed using SPSS software package (IBM SPSS Statistics 20.0, Chicago, Illinois), unless stated otherwise.

RESULTS

Among the total of 208 patients included in the PACIFIC study, coronary CTA images of 157 (75%) were fully evaluable by FFR_{CT} (3-vessel) and were used for the primary patient-based analysis. For 180 (87%) coronary CTA datasets, FFR_{CT} could be assessed at least in part. Altogether, 505 (83%) vessels could be evaluated by FFR_{CT} and were used for the primary vessel-based comparative analysis. Baseline characteristics of the study population are previously reported and therefore listed in Online Table 1 (14). In brief, patient age averaged 58.7 ± 8.5 years, 99 (63%) were male, and 71 (45%) patients were found to have significant CAD as defined by ICA with an FFR ≤0.80 or stenosis >90%. Coronary CTA assessment characteristics are shown in **Table 1**. Whereas failed FFR_{CT} analysis predominantly concerned the right coronary artery (51 of 107 unevaluable vessels, 48%), most frequent reasons for unevaluable datasets were related to relatively higher heart rates such as motion (84%) and misalignment (18%), next to noise (12%) and high calcification burden (10%). Occluded arteries were present in 11% of fully evaluable cases, compared to 4% in non-fully evaluable cases (p = 0.17). Although image quality varied, numbers of unevaluable datasets were 1 (0.5%) for coronary CTA, 2 (1.0%) for SPECT, and 0 (0%) for PET, next to 0 (0%) failed coronary CTA, 2 (1.0%) failed SPECT, and 4 (1.9%) failed PET scanning procedures due to technical issues or claustrophobia. Noninvasive test results were positive in 100 (64%) patients for FFR_{CT}, 90 (57%) patients for coronary CTA, 49 (31%) patients for SPECT, and 73 (47%) for PET (**Table 2**). **Figure 1** illustrates typical imaging findings for the currently tested modalities.

PER-VESSEL DIAGNOSTIC PERFORMANCE OF FFR_{CT}, CORONARY CTA, SPECT, AND PET FOR DIAGNOSING HEMODYNAMICALLY SIGNIFICANT CAD. Per-vessel diagnostic performances of all imaging modalities for

the detection of FFR-defined significant CAD in the primary analysis group (n = 505) are displayed in Table 3. As demonstrated in the Central Illustration and Figure 2A, the AUC for FFR_{CT} was 0.94 (95% CI: 0.92 to 0.96), and significantly higher than coronary CTA alone (0.83; 95% CI: 0.80 to 0.86; p < 0.001), SPECT (0.70; 95% CI: 0.65 to 0.74; p < 0.001), and PET (0.87; 95% CI: 0.83 to 0.90; p < 0.001). Diagnostic accuracy of FFR_{CT} (87%) was also higher than coronary CTA (79%) and PET (80%), but comparable with SPECT (82%). Sensitivity for FFR_{CT} (90%) was higher than any of the other modalities, whereas specificity for FFR_{CT} (86%) was comparable with coronary CTA and PET, yet lower than SPECT. The AUC for combined FFR_{CT} and coronary CTA was 0.95 (p = 0.051 compared with FFR_{CT} alone). Whereas selective FFR_{CT} assessment in case of coronary CTA stenosis >25% and >50% resulted in diagnostic accuracies of 88% and 86%, respectively.

PER-PATIENT DIAGNOSTIC PERFORMANCE OF FFR_{CT}, CORONARY CTA, SPECT, AND PET FOR DIAGNOSING HEMODYNAMICALLY SIGNIFICANT CAD. Detailed diagnostic performances of FFR_{CT} and the comparison with other noninvasive modalities on a per-patient level in the primary analysis group (n = 157) are also shown in Table 3. As shown in Figure 2B, discriminatory power for FFR_{CT} in terms of AUC was 0.92 (95% CI: 0.87 to 0.96), which was significantly greater than coronary CTA alone (0.81; 95% CI: 0.74 to 0.87; p = 0.002) and SPECT (0.75; 95% CI: 0.67 to 0.81; p < 0.001), but comparable to PET (0.91; 95% CI: 0.85 to 0.95; p = 0.559). Diagnostic accuracy of FFR_{CT} (78%), however, was comparable with coronary CTA alone (76%) and SPECT (78%), but was significantly lower than PET (88%). Selective FFR_{CT} assessment following coronary CTA stenosis >25% and >50% resulted in diagnostic accuracies of 84% and 83%, respectively (Table 2). The AUC for combined FFR_{CT} and coronary CTA was 0.95 (p = 0.053 compared with FFR_{CT} alone).

DIAGNOSTIC PERFORMANCES OF IMAGING MODALITIES FOR SIGNIFICANT CAD WITH AN INTENTION-TO-DIAGNOSE. Using the entire cohort of patients (n = 208) and vessels (n = 612), including nonevaluable vessels, an intention-to-diagnose analysis resulted in diagnostic performances as reported in Table 4 and Figure 3. Vessel-based AUC was equal among FFR_{CT} (AUC: 0.83), coronary CTA (AUC: 0.80; p = 0.261), and PET (AUC: 0.86; p = 0.157), but was lower for SPECT (AUC: 0.68; p < 0.001). Per-vessel and -patient AUC for combined FFR_{CT} and coronary CTA were 0.88 and 0.87, respectively (p < 0.001 and p = 0.001 compared with FFR_{CT} alone). There were no significant differences with regard to overall per-vessel diagnostic accuracy. However, FFR_{CT} showed the highest per-vessel sensitivity (92%) as opposed to the lowest specificity (70%). Per-patient AUC and diagnostic accuracy were comparable between FFR_{CT} (0.79 and 70%, respectively), coronary CTA (0.76 and 74%; p = 0.327 and p = 0.341, respectively), and SPECT (0.74 and 76%, p = 0.087 and p = 0.266, respectively), but were outperformed by PET (0.90 and 86%; p = 0.005 and p < 0.001, respectively). Per-patient sensitivity of FFR_{CT} (97%) was similar to coronary CTA, but higher than SPECT and PET. Conversely, specificity of FFR_{CT} (47%) was significantly inferior to each of the other modalities.

TABLE 2 Distribution of Noninvasive Imaging Results According to FFR-Based Subgroups

	FFR <0.70 (n = 56)	FFR 0.70–0.80 (n = 15)	FFR 0.80–0.90 (n = 52)	FFR >0.90 (n = 34)
FFR_{CT} (n = 157)				
FFR_{CT}≤0.80	55 (98)	13 (87)	27 (52)	5 (15)
FFR_{CT}	0.57 ± 0.10	0.72 ± 0.08	0.80 ± 0.08	0.85 ± 0.05
FFR_{CT}≤0.80 and stenosis>25%	54 (96)	13 (87)	17 (33)	4 (12)
FFR_{CT}≤0.80 and stenosis>50%	50 (89)	9 (60)	11 (21)	4 (12)
CCTA (n = 157)				
Stenosis >50%	51 (91)	11 (73)	19 (37)	9 (27)
Stenosis >70%	45 (80)	6 (40)	14 (27)	8 (24)
CAC score	421 (177–837)	487 (197–858)	96 (7–327)	5 (0–84)
SPECT (n = 157)				
SDS≥2	42 (75)	1 (7)	5 (10)	1 (3)
SDS	5 (0–10)	0 (0–0)	0 (0–0)	0 (0–0)
SSS	6 (0–12)	0 (0–0)	0 (0–0)	0 (0–0)
PET (n = 154)				
hMBF≤2.30	51 (94)	11 (73)	7 (14)	4 (12)
hMBF	1.55 ± 0.67	2.41 ± 0.68	3.42 ± 1.06	3.59 ± 0.92
CFR	1.65 ± 0.68	2.57 ± 0.65	2.98 ± 0.90	3.12 ± 0.89

Values are n (%), mean ± SD, or median (interquartile range).

CAC = coronary artery calcification; CAD = coronary artery disease; CFR = coronary flow reserve; CTA = computed tomography angiography; FFR = fractional flow reserve; FFR_{CT} = fractional flow reserve derived from computed tomography; hMBF = hyperemic myocardial blood flow; PET = positron emission tomography; SDS = summed difference score; SSS = summed stress score; SPECT = single-photon emission computed tomography.

CORRELATION OF FFR_{CT} AND INVASIVE FFR. Per-vessel FFR_{CT} values showed a good correlation with invasive FFR measures, Pearson's and Spearman's correlation coefficients were 0.80 and 0.67, respectively, p < 0.001 for both (Figure 4A). FFR_{CT} and FFR values were concordant in 87%, whereas 10% showed FFR_{CT} positive but FFR negative results, and 3% vice versa. Bland-Altman analysis indicated an underestimation of FFR_{CT} compared with FFR (mean difference, 0.05 ± 0.10; p < 0.001) (Figure 4B). According to subgroups of FFR_{CT} <0.60, 0.60 to 0.80, and >0.80, mean difference was 0.03 ± 0.11, 0.04 ± 0.15, 0.05 ± 0.08, respectively, with a significant overall intergroup difference (p < 0.001) using the analysis of

FIGURE 1 Case Example of Typical Noninvasive Imaging Results

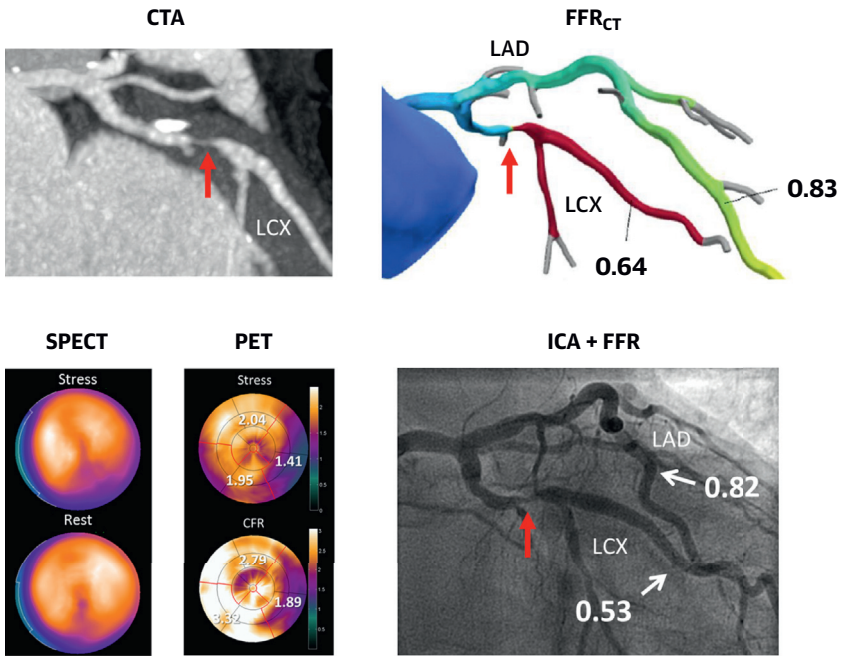

Representative imaging results of a 57-year old male with typical angina and a history of smoking. Multiplanar reformat of a coronary CTA demonstrating obstructive stenosis of the proximal LCX artery and a corresponding reduced FFR$_{CT}$ value of 0.64, next to a FFR$_{CT}$ value of 0.83 for the LAD artery. Myocardial perfusion imaging with SPECT and PET show, respectively, a reversible defect and a diminished stress MBF and CFR in the inferolateral territory. ICA with FFR measurements confirm the obstructive lesion and detrimental FFR value of 0.53 in the LCX. CTA = computed tomography angiography; CFR = coronary flow reserve; FFR = fractional flow reserve; FFR$_{CT}$ = fractional flow reserve calculated from computed tomography; ICA = invasive coronary angiography; LAD = left anterior descending; LCX = left circumflex; MBF = myocardial blood flow; PET = positron emission tomography; SPECT = single-photon emission computed tomography.

TABLE 3 Diagnostic Performance for the Detection of CAD of the Primary Analysis Group

	FFR$_{CT}$	Coronary CTA	p Value*	SPECT	p Value*	PET	p Value*
Per vessel (n = 505)							
Sensitivity	90 (84-95)	68 (60-76)	<0.001	42 (34-50)	<0.001	81 (72-87)	0.030
Specificity	86 (82-89)	83 (79-87)	0.386	97 (94-98)	<0.001	76 (69-82)	0.098
PPV	65 (57-73)	57 (48-66)	0.016	82 (71-89)	0.191	61 (52-69)	0.021
NPV	96 (92-98)	86 (81-90)	<0.001	80 (75-85)	<0.001	91 (86-94)	0.023
Diagnostic accuracy	87 (84-90)	79 (75-83)	0.002	82 (78-86)	0.084	80 (75-84)	0.004
AUC	0.94 (0.92-0.96)	0.83 (0.80-0.86)	<0.001	0.70 (0.65-0.74)	<0.001	0.87 (0.83-0.90)	<0.001
Per patient (n = 157)							
Sensitivity	96 (88-99)	87 (77-94)	0.146	61 (48-72)	<0.001	90 (80-96)	0.289
Specificity	63 (52-73)	67 (57-77)	0.585	93 (85-97)	<0.001	87 (78-93)	0.001
PPV	68 (62-74)	69 (58-78)	0.829	88 (76-94)	0.005	85 (76-91)	0.002
NPV	95 (85-98)	87 (76-94)	0.127	74 (68-79)	0.001	91 (84-96)	0.394
Diagnostic accuracy	78 (70-84)	76 (69-83)	0.878	78 (71-85)	1.000	88 (82-93)	0.012
AUC	0.92 (0.87-0.96)	0.81 (0.74-0.87)	0.002	0.75 (0.67-0.81)	<0.001	0.91 (0.85-0.95)	0.559

Values are proportions in % (95% confidence interval). *p values concern comparisons with FFR$_{CT}$.

AUC = area under the receiver operating characteristic curve; NPV = negative predictive value; PPV = positive predictive value; other abbreviations as in Table 2.

CENTRAL ILLUSTRATION **Discriminative Ability of Imaging Modalities for the Detection of Per-Vessel Fractional Flow Reserve-Defined Ischemia**

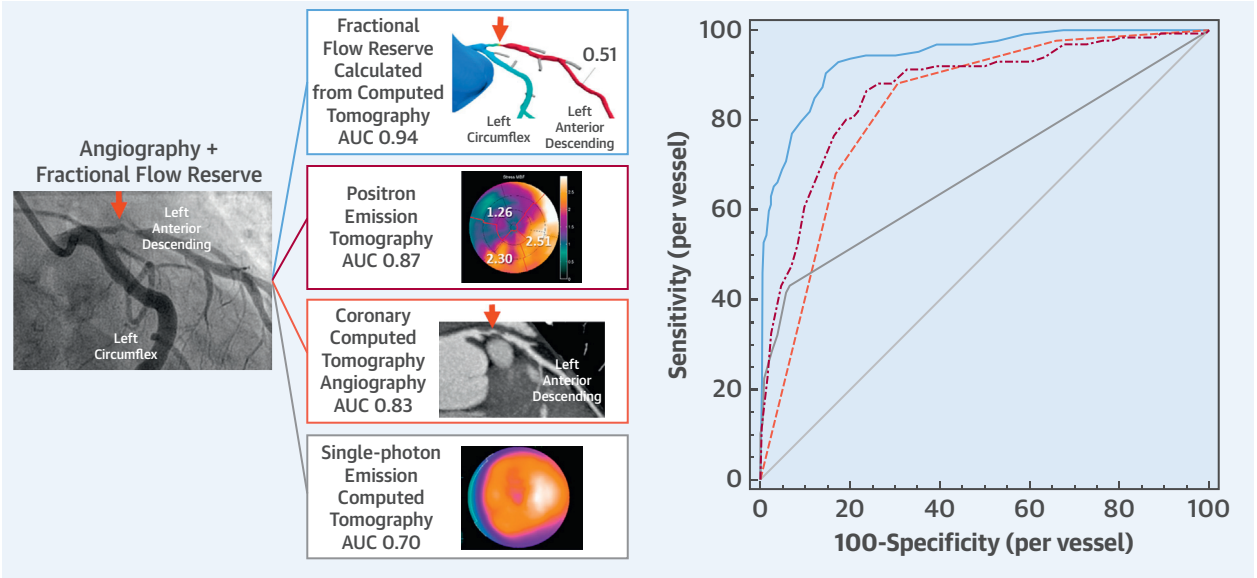

Driessen, R.S. et al. J Am Coll Cardiol. 2019;73(2):161–73.

Significance of stable coronary artery disease, as defined by invasive FFR, was prospectively tested with several noninvasive imaging modalities. Each patient underwent FFR_{CT}, PET, coronary CTA, SPECT, and ICA with FFR, regardless of imaging results as illustrated by the typical imaging findings of a severe left anterior descending artery stenosis in the **colored boxes. Curves with corresponding colors** indicate that FFR_{CT} demonstrated the greatest AUC for the detection of per-vessel ischemia. CTA = coronary computed tomography angiography; FFR = fractional flow reserve; FFR_{CT} = fractional flow reserve calculated from computed tomography; ICA = invasive coronary angiography; PET = positron emission tomography; SPECT = single-photon emission computed tomography.

variance test. In comparison, the Spearman's correlation with invasive FFR measures and (semi)quantitative coronary CTA stenosis, SPECT SDS, and PET MBF, were 0.55, 0.42, and 0.50, respectively. Accordingly, Online Figures 1 and 2 illustrate the relationship between PET and SPECT with FFR_{CT}.

DISCUSSION

In the present PACIFIC substudy of patients with suspected stable CAD, FFR_{CT} values strongly correlated with invasively derived FFR, which resulted in a high diagnostic performance (**Central Illustration**) even though, in line with previous reports, measured FFR_{CT} values were systematically lower than invasive FFR values. When images were of sufficient quality to analyze FFR_{CT}, it showed an improved per-vessel and -patient diagnostic discriminative ability compared with coronary CTA, SPECT, and PET in terms of AUC, except for per-patient analysis with PET. However, intention-to-diagnose analysis, including coronary CTA images nonevaluable for FFR_{CT}, diluted the incremental value of FFR_{CT} resulting in a lower per-patient AUC than PET. The current results represent the first true head-to-head comparison of the functional FFR_{CT} assessment derived from standard coronary CTA against more traditional functional imaging with SPECT and PET. Our findings support the use of FFR_{CT} in clinical practice, taking into account an anticipated increase of FFR_{CT} analyzability, whereas current multisociety guidelines do not advocate the use of any specific imaging modality (4,5).

DIAGNOSTIC PERFORMANCE OF FFR_{CT}. This study extends findings from 3 previous major FFR_{CT} studies regarding diagnostic performance as well as feasibility (11–13). Compared with results from the DeFACTO (Determination of Fractional Flow Reserve by Anatomic Computed Tomographic Angiography) study (12), the PACIFIC FFR_{CT} study showed a remarkably higher per-vessel diagnostic performance with an improved diagnostic accuracy from 69% towards 87%, despite only a slightly higher per-patient sensitivity and moderately increased specificity. Conversely, in comparison with results of the more

FIGURE 2 Discriminative Ability of Imaging Modalities for the Detection of Significant Coronary Artery Disease on a Per-Vessel and Per-Patient Basis for Primary Analysis

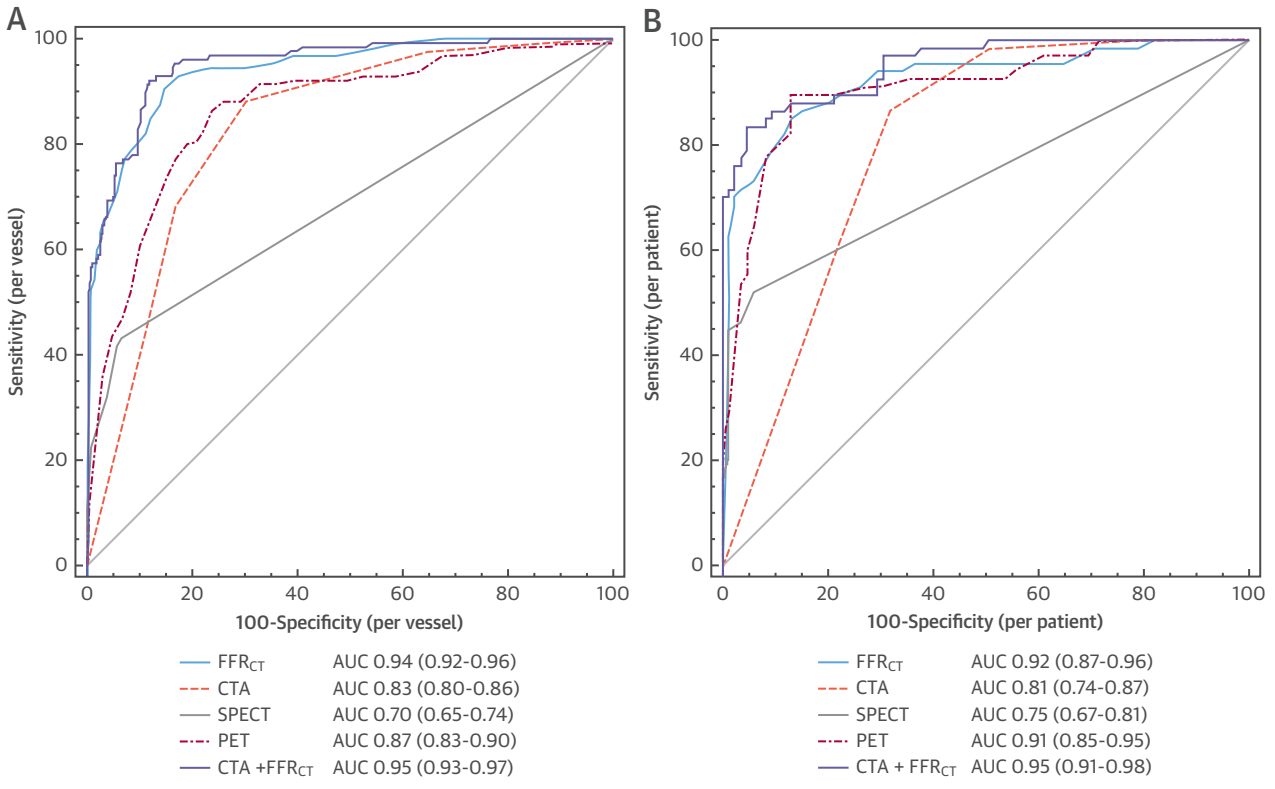

Receiver-operating characteristic curve analysis with corresponding area under the curves and 95% confidence intervals displaying the per-vessel **(A)** and per-patient **(B)** performance of FFR_{CT}, coronary CTA, SPECT, and PET compared with invasive FFR for the diagnosis of ischemia. AUC = areas under the receiver-operating characteristic curve; other abbreviations as in Figure 1.

TABLE 4 Diagnostic Performance for the Detection of CAD on an Intention-to-Diagnose Basis

	FFR_{CT}	Coronary CTA	p Value*	SPECT	p Value*	PET	p Value*
Per vessel (n = 612)							
Sensitivity	92 (86-96)	70 (62-77)	<0.001	40 (32-48)	<0.001	80 (73-86)	0.004
Specificity	70 (65-75)	78 (74-82)	0.005	96 (94-98)	<0.001	76 (69-81)	0.013
PPV	52 (45-60)	52 (45-60)	0.727	81 (71-88)	<0.001	61 (53-68)	0.134
NPV	96 (92-98)	86 (82-90)	<0.001	80 (75-84)	<0.001	91 (87-94)	0.015
Diagnostic accuracy	77 (73-80)	76 (73-80)	1.000	81 (78-84)	0.238	80 (77-83)	0.355
AUC	0.83 (0.79-0.86)	0.80 (0.77-0.84)	0.261	0.68 (0.64-0.72)	<0.001	0.86 (0.83-0.89)	0.157
Per patient (n = 208)							
Sensitivity	97 (91-99)	89 (81-95)	0.092	55 (45-66)	<0.001	87 (78-93)	0.022
Specificity	47 (38-57)	61 (51-70)	0.028	94 (88-97)	<0.001	86 (78-92)	<0.001
PPV	60 (56-64)	65 (60-70)	0.110	88 (78-94)	<0.001	83 (76-89)	<0.001
NPV	95 (85-98)	87 (79-93)	0.150	71 (67-76)	<0.001	89 (82-93)	0.184
Diagnostic accuracy	70 (63-76)	74 (67-79)	0.341	76 (70-82)	0.266	86 (81-91)	<0.001
AUC	0.79 (0.73-0.85)	0.76 (0.69-0.81)	0.327	0.74 (0.67-0.80)	0.087	0.90 (0.85-0.93)	0.005

Values are proportions in % (95% confidence interval). *p values concern comparisons with FFR_{CT}.
Abbreviations as in Tables 2 and 3.

FIGURE 3 Discriminative Ability of Imaging Modalities for the Detection of Significant Coronary Artery Disease on a Per-Vessel and Per-Patient Basis for Intention-to-Diagnose Analysis

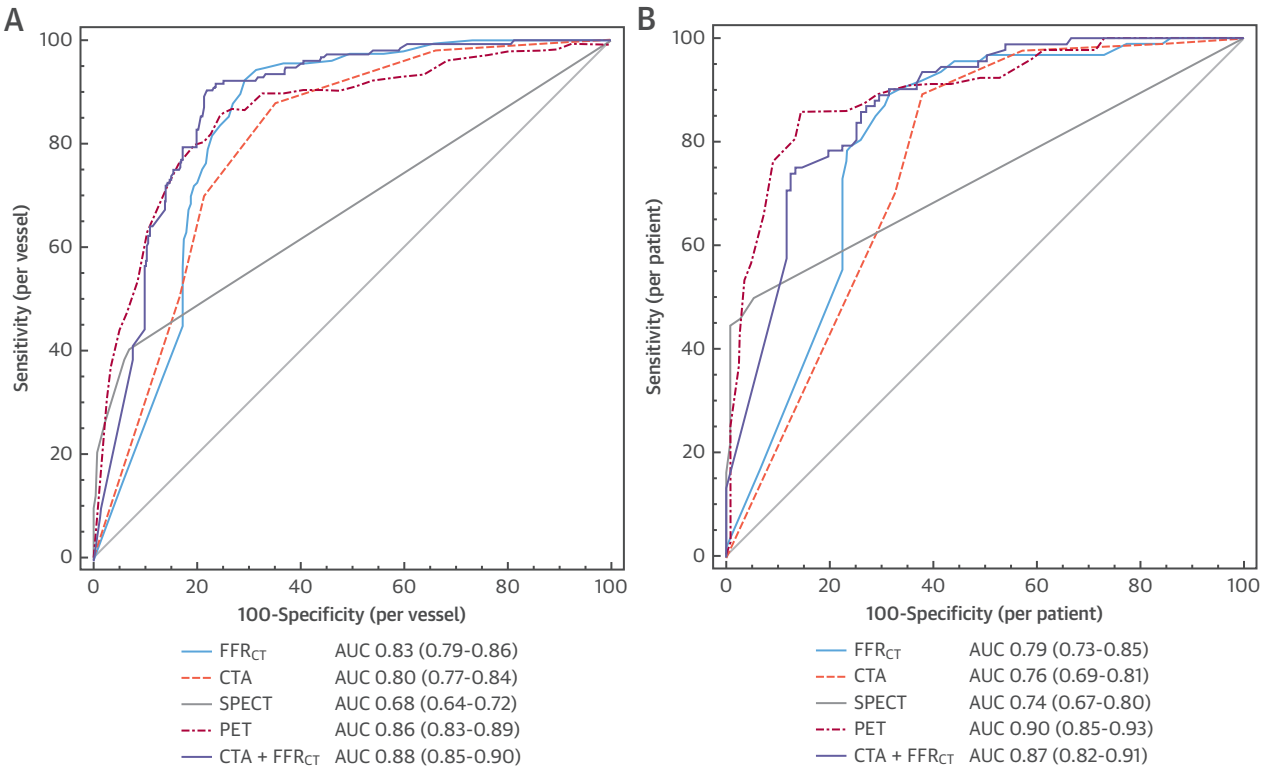

Receiver-operating characteristic curve analysis with corresponding area under the curves and 95% confidence intervals displaying the per-vessel **(A)** and per-patient **(B)** performance of FFR_{CT}, coronary CTA, SPECT, and PET compared with invasive FFR for the diagnosis of ischemia. Abbreviations as in Figures 1 and 2.

recent NXT (Analysis of Coronary Blood Flow Using CT Angiography: Next Steps) trial (13), per-vessel diagnostic performance results were particularly similar between both studies, resulting in the numerical highest accuracy for PACIFIC (86% vs. 87%). Because of its direct impact on diagnostic parameters in general, some differences between the current study and previous work may in part be due to the prevalence of FFR-defined significant CAD (45% for PACIFIC, against 51% for DeFACTO and 32% for NXT). Another dissimilarity between previous dedicated FFR_{CT} trials may be that patients in the PACIFIC trial underwent all imaging in a prospective manner after study inclusion without any of the noninvasive imaging tests already performed, and all coronary arteries were interrogated by FFR regardless of imaging results. Therefore, the current results reflect a genuine real-world performance of each of the modalities without potential inclusion bias, which might occur when patients are included after an initial test is performed and deemed suitable for study purposes. Furthermore, the present study showed a strong performance of FFR_{CT} analysis, and the superior performance compared with coronary CTA reading was significant on a per-vessel level yet limited on a per-patient level. This reduced incremental value of FFR_{CT} over coronary CTA in comparison with previous studies seems to be more related to the previously reported poor to moderate performance of coronary CTA than the altered performance of FFR_{CT} itself. The reason for the improved diagnostic accuracy of coronary CTA in the PACIFIC study (76%) compared with both the DeFACTO (64%) and NXT (53%) trials remains unknown, but improved scanner characteristics might play a role next to patient preparation and core laboratory reading. Still, most diagnostic parameters improved for FFR_{CT} in the current analysis, even with a proper performance of coronary CTA. In line with DeFACTO but in contrast to the NXT results, there was no marked increase in

FIGURE 4 Correlation and Bland-Altman Plots of FFR and FFR_{CT}

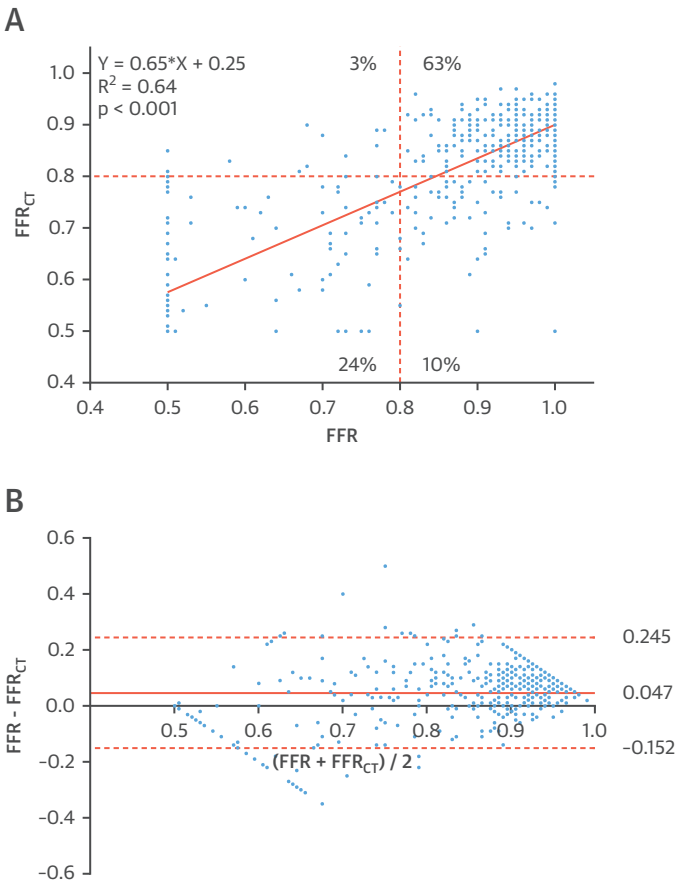

Scatterplot illustrating the quantitative relationship between FFR and FFR_{CT} **(A)**. Bland-Altman plot showing a systemic underestimation of FFR_{CT} as compared with FFR **(B)**. The mean difference is represented by the **solid orange line** with the 95% limits of agreement represented by the **dashed orange lines**. Abbreviations as in Figure 1.

specificity when FFR_{CT} was compared with coronary CTA alone, yet rather an increase in sensitivity. These altered sensitivity/specificity distributions could possibly be explained by the aforementioned differences in inclusion method and prevalence of disease, which resembles DeFACTO more than NXT, and is in line with the underestimation of FFR_{CT} values (Figure 4B). Another major difference from other studies that could explain some different findings is that in the PACIFIC trial, all vessels were measured with FFR, regardless of visual stenosis severity. As can be appreciated from Table 2, in the distinctly abnormal subgroup with FFR <0.70, all imaging modalities showed high rates of abnormal test results (range 75% to 98%). Interestingly, in the subgroup with minimally abnormal FFR values (0.70 to 0.80), SPECT showed almost no abnormal test results (7%) in contrast to the other imaging modalities (range 73% to 87%). This might partly explain the relatively low sensitivity of SPECT, but should be interpreted in context of previous optimal cutoff value derivation for PET and FFR_{CT} using invasive FFR values, which was not done for SPECT with FFR (10,17). In the subgroup with evidently normal FFR values (>0.90), coronary CTA still showed a relatively high prevalence of significant stenosis, reflecting the relatively low PPV. Furthermore, combined FFR_{CT} and coronary CTA stenosis severity showed a shift of slightly reduced positive test results in abnormal FFR cases but a more pronounced reduction of false positive results, which lead to a slightly enhanced AUC (Figures 2 and 3). As such, there seems to be additional value of FFR_{CT} analysis after visual coronary CTA stenosis assessment, which still might the be most convenient route in clinical practice.

CLINICAL APPLICABILITY OF FFR_{CT} COMPARED WITH MPI. In total, 83% of all vessels could be evaluated by FFR_{CT}, resulting in 75% fully evaluable datasets and 87% at least partly evaluable datasets. This drop-out rate resembles previous findings and remains a substantial issue in clinical practice. Interestingly, coronary calcification burden had only a minor impact on evaluability as reflected by small differences of median CAC scores between evaluable and nonevaluable images (Table 1). This is in line with a previous study by Norgaard et al. (19), and supports the potential of FFR_{CT} even in patients with high calcified plaque burden. Conversely, higher heart rates, additional administration of beta-blockers, and retrospective acquisition were shown to be predictive of nonevaluable CT scans. As such, an optimal use of FFR_{CT} in clinical practice appears to be greatly dependent on high-quality images as a result of adequate pre-scan medication and low heart rates, next to high-quality scanners and acquisition protocols. MPI with SPECT or PET, however, is usually not bothered by variable heart rates. A drawback of perfusion imaging, on the other hand, is the need of pharmacological stress or exercise, which can be simply simulated with FFR_{CT} from resting images (10). Of note, results of these tests provide essentially different information, as coronary CTA predominantly assesses epicardial coronary disease, whereas MPI evaluates the entire vascular bed including epicardial and microvascular function. As such, current European and American guidelines do not favor any specific test in general, but leave the choice of

modality to patient characteristics, next to local availability, clinical question asked, radiation exposure, and costs (4,5). Still, most guidelines recommend the use of stress imaging in intermediate- to high-risk patients because of the large body of evidence that ischemia-guided revascularization trumps anatomical-guided treatment with regard to improved outcome (9). Recently updated National Institute of Health and Care Excellence guidelines, however, advocate for coronary CTA as the initial test in patients with suspected CAD, regardless of pre-test likelihood of disease (20). In this regard, a large body of evidence exists for the prognostic value of both standard coronary CTA and MPI (21–23). Such data is still lacking for FFR_{CT}, but intuitively, the combination of anatomical and functional data from coronary CTA with FFR_{CT} holds great potential in prognostic value. In fact, the recent PLATFORM (Prospective Longitudinal Trial of FFRct: Outcome and Resource Impacts) trial showed FFR_{CT} to be an effective gatekeeper in clinical work-up as reflected by reducing the number of unnecessary invasive coronary angiography in up to 61% of patients without compromising clinical outcome (24,25). Additionally, the potential of FFR_{CT}-guided revascularization was shown by Curzen et al. (26) with a change in treatment strategy of 36% of patients suspected of having CAD. However, larger studies with a longer follow-up of these low-risk patients are eagerly awaited to provide more insights in the prognostic value of FFR_{CT}. Furthermore, notwithstanding the high diagnostic agreement in terms of concordancy, the distinct scatter of actual estimated FFR_{CT} values as displayed in **Figure 4** could be clinically relevant and necessitates careful interpretation.

STUDY LIMITATIONS. The present study was a post hoc subanalysis of the previously reported PACIFIC study. Although the drop-out rate is expected to decrease with future improvement of CT scanner possibilities, software updates, and optimized patient preparation, a considerable proportion of 17% of vessels were qualified as nonevaluable by FFR_{CT} and were excluded from the primary analysis. Therefore, a subsequent intention-to-diagnose analysis with all datasets was performed, which resulted in an ample shift of diagnostic performances in an unfavorable way for FFR_{CT}. As such, a truly prospective comparison of imaging modalities is warranted with prespecified optimized CT acquisition. Of note, in a recent large registry, the acceptance rate for FFR_{CT} was 95% (27). Although the present results would likely not have been substantially different if FFR_{CT} extraction had been performed blinded to the knowledge of the pressure wire position, it could have potentially enhanced the quantitative relationship with FFR. Accordingly, the continuous nature of the results of FFR_{CT} may disadvantage modalities like coronary CTA and SPECT with limited categories of outcome results (**Figures 3 and 4**). Even so, definitions of ischemia of PET and SPECT were determined based on international guidelines, disregarding, however, the potential extent and depth of ischemia, which are of clinical validity. Using alternative thresholds for SPECT scoring such as 5% reversible perfusion defect, or using different outcome parameters for PET such as coronary flow reserve could alter current results. Whereas a widely available SPECT protocol and tracer were used, PET was performed with the less frequently used $[^{15}O]H_2O$ tracer. Hence, current results may not be extrapolated to the more commonly used tracers $[^{13}N]NH_3$ and Rubidium-82. It should, however, be emphasized that the results of the current analysis only apply to patients with a normal LVEF without a prior documented history of CAD. Furthermore, generalizability of present FFR_{CT} findings might be hampered by the relatively small sample size and the single-center study setup with the use of 1 specific coronary CTA acquisition protocol and scanner. Last, although it is believed that coronary CTA generally performs best in low-risk populations, the influence of current patient population with a relatively high prevalence of CAD is unknown, while patients with a documented history of CAD were excluded.

CONCLUSIONS

In this head-to-head comparative study, FFR_{CT} showed the highest diagnostic performance for vessel-specific ischemia, provided coronary CTA images were evaluable by FFR_{CT}. On an intention-to-diagnose basis, however, PET displays the highest diagnostic performance due to the relatively high rejection rate of FFR_{CT}. Further improvements in CT acquisition and reconstruction are needed to improve the evaluability rate of FFR_{CT} so the diagnostic performance could be similar to PET. Still, FFR_{CT} would be of value in clinical practice for the noninvasive evaluation of CAD, providing not only anatomic but also hemodynamic significance of coronary lesions.

ADDRESS FOR CORRESPONDENCE: Dr. Paul Knaapen, Department of Cardiology, VU University Medical Center, De Boelelaan 1117, 1081 HV Amsterdam, the Netherlands. E-mail: p.knaapen@vumc.nl. Twitter: @VumcAmsterdam.

PERSPECTIVES

COMPETENCY IN PATIENT CARE AND PROCEDURAL SKILLS: In patients with stable CAD and adequate image quality, FFR_{CT} provides superior functional assessment of coronary stenosis compared with coronary CTA, SPECT, or PET imaging.

TRANSLATIONAL OUTLOOK: Future studies should focus on enhancing CT image acquisition and reconstruction to improve the applicability of FFR_{CT} in clinical practice.

REFERENCES

1. Danad I, Szymonifka J, Twisk JWR, et al. Diagnostic performance of cardiac imaging methods to diagnose ischaemia-causing coronary artery disease when directly compared with fractional flow reserve as a reference standard: a meta-analysis. Eur Heart J 2017;38:991–8.

2. Hachamovitch R, Rozanski A, Shaw LJ, et al. Impact of ischaemia and scar on the therapeutic benefit derived from myocardial revascularization vs. medical therapy among patients undergoing stress-rest myocardial perfusion scintigraphy. Eur Heart J 2011;32:1012–24.

3. Patel MR, Peterson ED, Dai D, et al. Low diagnostic yield of elective coronary angiography. N Engl J Med 2010;362:886–95.

4. Montalescot G, Sechtem U, Achenbach S, et al. 2013 ESC guidelines on the management of stable coronary artery disease: the Task Force on the Management of Stable Coronary Artery Disease of the European Society of Cardiology. Eur Heart J 2013;34:2949–3003.

5. Fihn SD, Blankenship JC, Alexander KP, et al. 2014 ACC/AHA/AATS/PCNA/SCAI/STS focused update of the guideline for the diagnosis and management of patients with stable ischemic heart disease: a report of the American College of Cardiology/American Heart Association Task Force on Practice Guidelines, and the American Association for Thoracic Surgery, Preventive Cardiovascular Nurses Association, Society for Cardiovascular Angiography and Interventions, and Society of Thoracic Surgeons. J Am Coll Cardiol 2014;64:1929–49.

6. Meijboom WB, Meijs MF, Schuijf JD, et al. Diagnostic accuracy of 64-slice computed tomography coronary angiography: a prospective, multicenter, multivendor study. J Am Coll Cardiol 2008;52:2135–44.

7. Tonino PA, Fearon WF, De BB, et al. Angiographic versus functional severity of coronary artery stenoses in the FAME study fractional flow reserve versus angiography in multivessel evaluation. J Am Coll Cardiol 2010;55:2816–21.

8. Meijboom WB, van Mieghem CA, van PN, et al. Comprehensive assessment of coronary artery stenoses: computed tomography coronary angiography versus conventional coronary angiography and correlation with fractional flow reserve in patients with stable angina. J Am Coll Cardiol 2008;52:636–43.

9. Tonino PA, De BB, Pijls NH, et al. Fractional flow reserve versus angiography for guiding percutaneous coronary intervention. N Engl J Med 2009;360:213–24.

10. Taylor CA, Fonte TA, Min JK. Computational fluid dynamics applied to cardiac computed tomography for noninvasive quantification of fractional flow reserve: scientific basis. J Am Coll Cardiol 2013;61:2233–41.

11. Koo BK, Erglis A, Doh JH, et al. Diagnosis of ischemia-causing coronary stenoses by noninvasive fractional flow reserve computed from coronary computed tomographic angiograms. Results from the prospective multicenter DISCOVER-FLOW (Diagnosis of Ischemia-Causing Stenoses Obtained Via Noninvasive Fractional Flow Reserve) study. J Am Coll Cardiol 2011;58:1989–97.

12. Min JK, Leipsic J, Pencina MJ, et al. Diagnostic accuracy of fractional flow reserve from anatomic CT angiography. JAMA 2012;308:1237–45.

13. Norgaard BL, Leipsic J, Gaur S, et al. Diagnostic performance of noninvasive fractional flow reserve derived from coronary computed tomography angiography in suspected coronary artery disease: the NXT trial (Analysis of Coronary Blood Flow Using CT Angiography: Next Steps). J Am Coll Cardiol 2014;63:1145–55.

14. Danad I, Raijmakers PG, Driessen RS, et al. Comparison of coronary CT angiography, SPECT, PET, and hybrid imaging for diagnosis of ischemic heart disease determined by fractional flow reserve. JAMA Cardiol 2017;2:1100–7.

15. Abbara S, Blanke P, Maroules CD, et al. SCCT guidelines for the performance and acquisition of coronary computed tomographic angiography: a report of the society of Cardiovascular Computed Tomography Guidelines Committee: Endorsed by the North American Society for Cardiovascular Imaging (NASCI). J Cardiovasc Comput Tomogr 2016;10:435–49.

16. LeCun Y, Bengio Y, Hinton G. Deep learning. Nature 2015;521:436–44.

17. Danad I, Uusitalo V, Kero T, et al. Quantitative assessment of myocardial perfusion in the detection of significant coronary artery disease: cutoff values and diagnostic accuracy of quantitative [(15)O]H2O PET imaging. J Am Coll Cardiol 2014;64:1464–75.

18. DeLong ER, DeLong DM, Clarke-Pearson DL. Comparing the areas under two or more correlated receiver operating characteristic curves: a nonparametric approach. Biometrics 1988;44:837–45.

19. Norgaard BL, Gaur S, Leipsic J, et al. Influence of Coronary Calcification on the Diagnostic Performance of CT Angiography Derived FFR in Coronary Artery Disease: A Substudy of the NXT Trial. J Am Coll Cardiol Img 2015;8:1045–55.

20. National Institute for Health and Care Excellence. Chest Pain of Recent Onset: Assessment and Diagnosis of Recent Onset Chest Pain or Discomfort of Suspected Cardiac Origin (Update). Clinical Guideline 95. London: National Institute for Health and Care Excellence, 2016.

21. Min JK, Berman DS, Dunning A, et al. All-cause mortality benefit of coronary revascularization vs. medical therapy in patients without known coronary artery disease undergoing coronary computed tomographic angiography: results from CONFIRM (COronary CT Angiography EvaluatioN For Clinical Outcomes: An InteRnational Multicenter Registry). Eur Heart J 2012;33:3088–97.

22. Douglas PS, Hoffmann U, Patel MR, et al. Outcomes of anatomical versus functional testing for coronary artery disease. N Engl J Med 2015;372:1291–300.

23. Shaw LJ, Berman DS, Maron DJ, et al. Optimal medical therapy with or without percutaneous coronary intervention to reduce ischemic burden: results from the Clinical Outcomes Utilizing Revascularization and Aggressive Drug Evaluation (COURAGE) trial nuclear substudy. Circulation 2008;117:1283–91.

24. Douglas PS, Pontone G, Hlatky MA, et al. Clinical outcomes of fractional flow reserve by computed tomographic angiography-guided diagnostic strategies vs. usual care in patients with suspected coronary artery disease: the

prospective longitudinal trial of FFR(CT): outcome and resource impacts study. Eur Heart J 2015;36:3359–67.

25. Douglas PS, De BB, Pontone G, et al. 1-Year outcomes of FFRCT-guided care in patients with suspected coronary disease: the PLATFORM Study. J Am Coll Cardiol 2016;68:435–45.

26. Curzen NP, Nolan J, Zaman AG, Norgaard BL, Rajani R. Does the routine availability of CT-derived FFR influence management of patients with stable chest pain compared to CT angiography alone? The FFRCT RIPCORD Study. J Am Coll Cardiol Img 2016;9:1188–94.

27. Kitabata H, Leipsic J, Patel MR, et al. Incidence and predictors of lesion-specific ischemia by FFRCT: learnings from the international ADVANCE registry. J Cardiovasc Comput Tomogr 2018;12:95–100.

KEY WORDS coronary artery disease, coronary computed tomography angiography, fractional flow reserve, myocardial perfusion imaging

APPENDIX For a supplemental table and figures, please see the online version of this paper.